# Development of a Hybrid Linear Motor for Conveyor Belts

M. Radosavac, L. Overmeyer


## ABSTRACT

In the field of warehousing belt conveyor systems are used to transport single piece goods and light bulk material. When using conventional drive systems the feed force has to be transmitted by frictional force over the driven pulley to the conveyor belt. As alternative drive principle, linear direct drives are characterized by direct force transmission from the motor to the conveyor belt instead of through the driven pulley. Thus, the belt tension and the belt stress from the motional resistance can be reduced significantly, which allows the usage of lighter and cost-efficient belts compared to conventional drive concepts. In this approach a linear direct drive system was developed which combines the advantages of the permanent magnet synchronous motor principle with those of reluctance motors. Simulation results with focus on the force progression from the motor to the secondary elements lead to the development and investigation of different mounting concepts for the secondary elements on the conveyor belt. Due to the high elongation characteristic of conveyor belts, alternative guidance concepts are necessary, because even slight geometrical deviation on the alignment of the mounted secondary elements lead to high frictional loss. Different guidance concepts were investigated and proven by measurements, which allow an estimation concerning the suitability of linear direct drive systems for conveyor belts.


## 1 INTRODUCTION

In the field of warehousing applications, product and piece goods are moved typically from a starting point to an ending point via conveyors. In a company, the technical resources of the material flow system perform the transportation task. The requirements nowadays for material flow systems become increasingly complex due to individual customer requests, shortened innovation cycles and an increasing diversity of product types. [1, 2]

The means of transportation used within the material flow system are divided into continuous conveyors – which include i.e. belt conveyors, vibratory conveyors as well as roller conveyors – and non-continuous conveyors, which include i.e. forklift trucks and gantry cranes. Continuous conveyors are used for the transportation of single piece goods and light bulk material. The conveyors work continuously over a longer period of time but can also operate in a clocked way. [3]

Due to their simple construction design, belt conveyors are widespread for continuous transportation tasks. They usually consist of a supporting framework, which is equipped with a deflection pulley at the inlet and a driven pulley at the outlet. The drive motor either is located inside the pulley or is attached to a gearbox, which in turn is connected to the driven pulley. [4] Figure 1 schematically shows the principle of the described belt conveyor. To move the conveyor belt, the entire feed force has to be transmitted by frictional connection over the driven pulley. The forces $F_1$ and $F_2$ indicate the corresponding force progression inside the conveyor belt, which is caused by the conventional drive principle. For visualization purposes, the forces are marked perpendicularly to their effective direction.

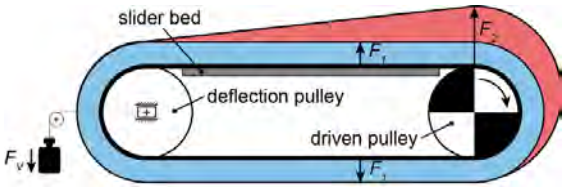


*Fig. 1 Conventional belt conveyor*

The appropriately high force $F_1$ results from the belt pretension, which is necessary to prevent the belt from slipping and to operate without interference at any loading condition. It is therefore set by adjusting the pulleys' axis distance by the force $F_V$. A further force $F_2$ results from the motional resistance because of moving the conveyor belt. The value of the force $F_2$ increases in the top-run in a linear way over the belt length towards the driven pulley and reaches its peak directly above that pulley, which shortly after drops down logarithmically. [5] For short-track timing conveyors the axis distance of the pulleys must be sufficient large, to ensure proper straight running behavior of the belt. Furthermore, the allowed tension force of the conveyor belt is a design criterion for the maximum belt conveyor length. To reach large conveying distances, either conveyor belts with high nominal strength or the distribution to multiple conveyors with shorter axis distances is necessary. [6] The creation of

continuous and constant frictional connection between the driven pulley and the conveyor belt is a critical point. Peak stress, i.e. during the start and stop procedure, can lead to alternating static and sliding friction, which results in oscillating, sudden movements of the conveyor belt. [7] This unwanted stick-slip-effect can be reduced by adding further driven pulleys to the system or by using special material combinations such as a rubberized driven pulley on the carrying side of the conveyor belt.

For the reduction of the conveyor belt stress, alternative drives are focus of current research. Figure 2 shows two possibilities for the application of distributed drive principles. Especially in the field of conveying bulk material over long distances, a large number of idlers is located as support in the top-run. In the first step of the investigations, these idlers are connected to a motor. Besides the driven pulley this enables the possibility to transmit the feed force additionally through the idlers over the whole conveyor belt length. As consequence, the driven pulley is relieved and the belt stress is reduced at the same time. The complete substitution of the driven pulley by driven idlers could lead to a cost-efficient and modular belt conveyor of the future. [8]

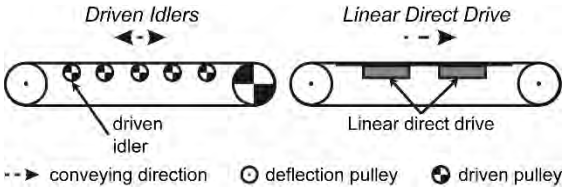


*Fig. 2 Distributed drive principles*

Linear direct drives constitute another alternative drive system. In contrast to conventional drive systems, here, the feed force results from the electro-magnetic field and is transmitted over the motor length directly into the conveyor belt without further mechanical transmission elements. In contrast to driven idlers, this drive principle is suitable for belt conveyors in warehousing applications that consists in the top-run of a slider bed. [9]

Figure 3 schematically depicts the force progression inside the conveyor belt resulting from the use of linear direct drives.

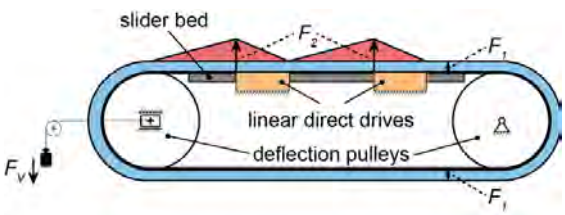


*Fig. 3 Belt conveyor with linear direct drive*

As consequence of the larger force transmission path, the conveyor belt pretension $F_1 \approx F_v$ can be reduced significantly compared to the conventional drive principle in figure 1. Furthermore, by comparison of force $F_2$ in fig. 1 and 3, the peak load, which occurs from the motional resistances can be reduced by using a linear direct drive system. As the peak load is lower, it is possible to use a lighter and more cost-efficient conveyor belt with a lower nominal strength for the same transportation task. The conventional drive concept shows limitations when dealing with longer distances as it requires conveyor belts with an increasing nominal strength, which also have a higher weight. Besides an appropriately high pretension, the necessary drive power increases as well. Concerning an economic operation, these cases often lead to a forced distribution to multiple conveyors with shorter sections. The use of several linear direct drives connected in series is therefore advantageous, as it is possible to use conveyor belts with a comparatively small nominal strength on long distances, which relativizes alternatives such as splitting into shorter sections. In addition, the proper straight running behavior of the belt on short-track timing conveyors is not a problem anymore, due to the drive principle, which is equipped with a forced guidance between conveyor belt and motor. Linear direct drive systems allow the realization of shorter, space-saving and timing conveyors to perform highly dynamic tasks such as piling up or increasing the distance between single transport units. [10]

## 2 HYBRID LINEAR MOTOR AS DRIVE OPTION

Concerning warehousing applications, linear direct drives are primarily used for sorter drives. Sorter are systems or facilities, which identify piece goods arriving in an unorganized way along a distribution conveyor line according a to a sort criterion and subsequently distribute the goods to several collection points. [4] Applications for linear direct driven belt conveyors have been previously investigated on the basis of asynchronous drives. [9] However, these applications are characterized by low efficiency and a high amount of heat induction into the conveyor belt.

Within the scope of a DFG cooperation project of the Institute of Transport and Automation Technology and the Institute for Drive Systems and Power Electronics of the Leibniz Universität Hannover, a linear direct drive system was developed for the use of conveyor belts in warehousing applications. In contrast to asynchronous drives, the use of the investigated

synchronous drive, which consists of permanent magnet materials, shows several advantages: Besides the omission of electrical conductors inside the rotor, which leads to the elimination of additional heat input, a higher efficiency can be expected.

As drive concept, the principle of the hybrid motor has been investigated. The hybrid motor combines the advantages of the permanent-magnet-excited machines' high efficiency and the principles of reluctance motors. Concerning the hybrid motor, the permanent magnets can be mounted inside the static stator part of the motor. As a result, the secondary elements mounted at the conveyor belt only need to consist of soft magnetic materials. [11] Figure 4 depicts the design of the hybrid motor.

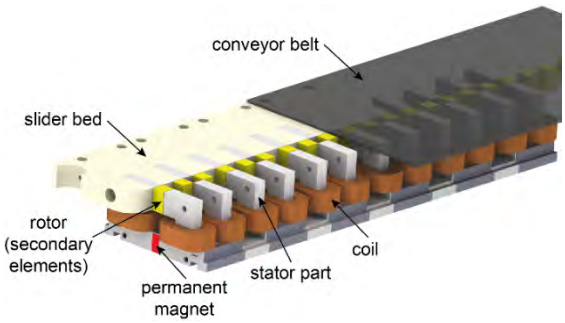


*Fig. 4 Design of the hybrid motor*

The permanent magnetic field is guided into the effective range of the motor with the help of a yoke in the shape of a double "U". The enhancement of the magnetic field and the creation of a moving electromagnetic field is realized by a concentrated winding. An appropriate frequency converter controls the current in the coils. This allows the user defined setting of the driven force and the direction of movement. For this machine type, a moving electromagnetic field, which is also interrelated with the permanent-magnet-excitation, is generated by applying current to the stand, which induces a force onto the secondary elements mounted at the conveyor belt. As a result of the flat construction, which is implemented in the slider bed, several linear direct drives can be installed along the conveyor line in order to minimize the conveyor belt tension force and to enable a transport without forced distribution to multiple conveyors with shorter sections. [11]

Due to the high prevalence of flexible conveyor belts in warehouse applications the focus of the investigation is laid on the integration of secondary elements into this type of belts for the drive concept of a hybrid motor.

For a successful linear motor operation the following two sub-goals are crucial and discussed in the following:

- Investigation of the force transmission path from the motor into the conveyor belt with the objective of an ideal mounting concept between secondary elements and conveyor belt
- Construction of a functional guidance system, which reduces the frictional influence between secondary elements and stator part to a minimum

## 3 INTERFACE: SECONDARY ELEMENTS AND CONVEYOR BELT

### 3.1 FORCE TRANSMISSION

The choice of an optimized conveyor belt, the mounting, the material as well as the geometrical outer shape of the secondary elements influence the operating performance of linear direct driven conveyor belts significantly. The design of long conveyor belts without distribution to multiple conveyors particularly requires a dimensioning concerning the force transmission in order to transfer the feed force generated by the motor on to the above positioned light bulk material and piece goods in the most direct and efficient way as possible.

In order to be able to depict the force transmission and progression as practical as possible, the finite element method (FEM) is used. The FEM is based on a decomposition of the examined continuum into individual elements. Afterwards, a solution can be calculated for each element, whose combination leads to an overall solution. Concerning a practical depiction of the conveyor belt, the multi scale approach is used, which is based on the analysis of elementary cells, in which the conveyor belt can be divided because of its periodic structure. [12] Figure 5 depicts the chosen conveyor belt consisting of an uncoated polymer fabric for the bottom side and an elastomer top layer for the carrying side, which is representative for warehousing applications.

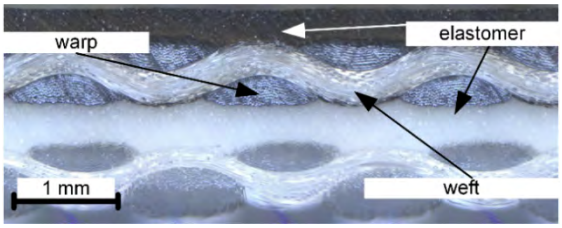


*Fig. 5 Intersection in the conveyor belt*

It clearly shows the periodic characteristic of the warp and weft threads in shape of a textile plain weave, which runs along the entire conveyor belt running side. The warp and weft threads themselves consist of 420 individual filaments each.

For the simulation of the force progression, the conveyor belt's shaping follows three steps according to the multi scale approach:

7 Microscale (elementary cell)

8 Mesoscale (cell with surrounding matrix)

9 Macroscale (complete structure)

In the smallest scale, the microscale, the focus is laid on the elementary cell, which includes the mechanical characteristics on the fiber layer. The basis of the model is information about the fiber geometry, i.e. the diameter and type of package, which orientate themselves at the geometric facts of the analyzed conveyor belt. The geometry, which is the result of the modeling process, is subsequently equipped with material laws, which are determined by material examination of the individual components. Test data of the conveyor belt manufacturer are available for this step. The calculation of the mechanical characteristics are carried out with the FEM.

In the mesoscale, which builds upon the microscale, a representative elementary cell is created, which includes the threads and the surrounding elastomer matrix. Thereby, the previously determined fiber characteristics are homogenized into a thread and written in as material laws into the geometric representation of the threads. Here, the waviness has to be considered as well as the occurring change of cross section and the local material orientations. The mechanical characteristics of the elastomer matrix can be determined with the help of tension tests by using the single components of the actual material. After that, the FEM calculation of the mechanical characteristics of all components in combination is conducted. Figure 7 shows the resulting model of the meso cell consisting of warp and weft threads, the intermediate layer, the top layer and the surrounding matrix.

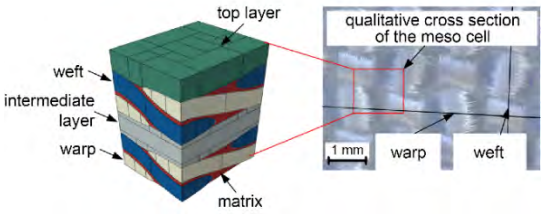


*Fig. 7 Model of the meso cell*

The FEM calculation of the meso cell allows the determination of the material characteristics of the superior macro scale. The repeated homogenization leads to a simplification of the geometry without risking the improper simplification of significant material characteristics. As for its dimension and the transported goods, the conveyor belt represents the mechanical case of a disk, which is an even load-bearing surface structure and is thus much thinner in comparison to the side length. Here, stress is only applied on the layer. Therefore, it is possible to model the conveyor belt as a shell element in the FEM. The conveyor belt modelling is achieved by comparing the stiffness between the model and the actual belt. The outcome of this test enables the depiction of the force progression from the motor into the conveyor belt when conveying a single piece good.

Due to the parametric design, all input and output parameters can be varied, which expands the range of conveyor scenarios.

Figure 8 shows the difference of the force transmission between the conventional drive and the linear direct drive when conveying a single piece good, which was the result of the FE analysis.

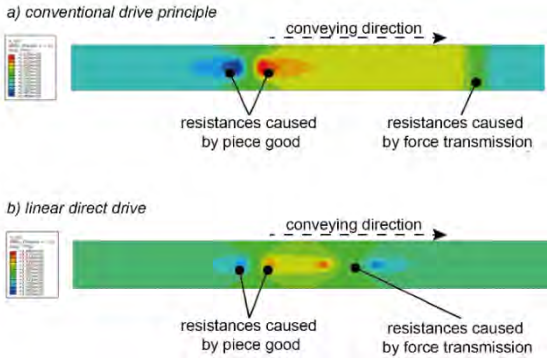


*Fig. 8 Qualitative progress of the force transmission into the conveyor belt*

Concerning the conventional drive (Figure 8a), constant stress is visible at the margins of the conveyor belt in the direction of transportation, which is caused by the conveyor belt pretension. In the area of the right deflective pulley, the drive force is transmitted, which is visible through the resistance caused by the drive force transmission. From this point on the conveyor belt tension increases and continues to do so up to the area of the single piece good's position on the left side. The resistance of the single piece good transportation causes a stress concentration in front of the piece good, whereas a reduction of local stress can be recognized in the area behind the piece good.

Concerning the linear direct drive (Figure 8b), the resistances of the single piece good create a progression similar to the conventional drive. Due to the force transmission, which is centric to the middle axis of the conveyor belt, a local stress concentration emerges after the drive in the transportation direction, while stress is

caused in the area in front of the drive, which is smaller than the preload.

The reason for this type of distribution can be seen in the principle of Saint-Venant, which describes the stress distribution within an object, which is strained with tensile stress at one margin. [13]

Figure 9 illustrates the principle with the help of an object fixed on one side. Thereby, a force is applied on the right end of the object, which is described by the stress condition $\sigma_0$.

Within a defined section, the stress distribution caused by the edge disturbances develops from a stress concentration in the immediate surrounding area of the force transmission into a constant stress distribution on to the entire cross section of the object.

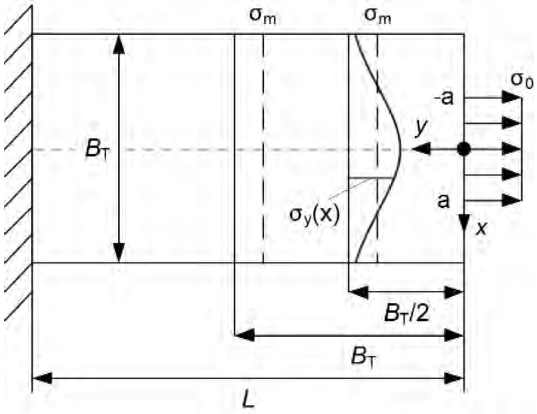


*Fig. 9 The principle of Saint-Venant [13]*

The length of the section, in which a stress homogenization takes place, is solely dependent on the width $B_T$ of the object and corresponds to the amount of the width with sufficient accuracy. This means that there is a constant stress distribution on to the entire cross section of the object, if the distance of the cross section to the point of force transmission is at least corresponding with the value of the object's width. Concerning the depicted object, it can be seen that its thickness is smaller than its width and that a constant stress condition is existent. Due to the analysis of the stress distribution caused by the force transmission, it can be concluded that the tension within the conveyor belt shows an even distribution after a length of the amount of $B_T$. Thus, it is possible to create a model of the stress distribution caused by the force transmission on the basis of the Saint-Venant principle. For an evaluation of the optimum force progression at the interface conveyor belt - secondary elements, three different types of force transmission are analyzed:

- Conventional drive: driven by the pulley
- Linear direct drive: secondary elements mounted by screws
- Linear direct drive: secondary elements sewn up at both sides with separate tension belt as intermediate layer

Figure 10 depicts the absolute values of the stress progression curve at the point of creation along the entire width of the conveyor belt.

This shows that the secondary elements mounted by screws causes a significantly stronger stress concentration in the conveyor belt than the other two concepts. The conventional drive shows a maximum tension of 4.98 % compared to the maximum tension in case of secondary elements mounted by screws. Concerning the secondary elements sewn up at both sides, the increase of the tension amounts to only 32.7 % compared to the maximum tension in the case where the secondary elements are mounted by screws.

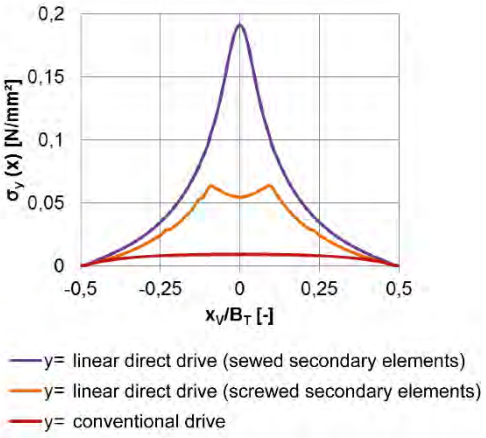


*Fig. 10 Stress progression caused by different force transmissions*

Concerning the secondary elements sewn up at both sides, the increase of the tension amounts to only 32.7 % compared to the maximum tension in the case where the secondary elements are mounted by screws. The two maxima on the right and left side of the conveyor belt's center can be ascribed to the force influences, which are applied on the conveyor belt through the seams on both sides. On the basis of these results the width ratio $k_B$ is defined, which relates the width of the force transmission $B_L$ to the width of the conveyor belt $B_T$.

$$k_B = \frac{B_L}{B_T}$$

The width ratio of the investigated mounting concepts and the conventional drive is calculated in Table 1.

Table 1 shows that a maximization of the width ratio $k_B$ is to be aspired to. As the width of the belt is constructively defined for its individual application, the width of the force transmission needs to be increased in order to positively influence the interface conveyor belt - secondary elements.

| Drive Concept | $B_L$ in mm | $B_T$ in mm | $k_B$ in (-) |
|---|---|---|---|
| Conventional | 500 | 500 | 1.000 |
| Linear direct drive (screwed) | 15 | 500 | 0.030 |
| Linear direct drive (sewed) | 91 | 500 | 0.182 |

*Tab. 1 Calculation of the width ratio*

## 3.2 MOUNTING CONCEPT

The interface secondary elements - conveyor belt is responsible for the transmission of the entire feed force from the linear direct drive to the conveyor belt. The following requirements are necessary for an interference-free operation:

- high width ratio $k_B$ (see previous section)
- material characteristics of the secondary elements: high electrical conductivity and high magnetic permeability
- preservation of the pole pitch of the linear direct drive
- temperature resistance up to 125 °C
- transmission of forces and torque

In order to achieve a high efficiency, it is preferable to use soft magnetic materials for the secondary elements, which provide high electrical conductivity and a high magnetic permeability. At the same time, a geometrical volume maximization of the object is to be aspired. Concerning the concept with the screwed secondary elements, drill holes lead to a reduction of the geometrical volume. Corresponding FE-analysis proves that a reduction of the overall feed force of the linear direct drive of about 23 % can be expected using a drilling diameter of 6 mm. The reason for this can be found in the reduction of the flow leading cross section of the secondary element.

Although the screw itself positively influences the flow leading in the practical case and thus enlarges the cross section, the iron of the secondary element will saturate in the area of the smallest available cross section. Moreover, the screw will not fill the drill hole completely.

The design of the linear direct drive gives a fixed pole pitch of 30 mm, which should be entirely considered, if possible in order to avoid a reduction of the efficiency. Flexible conveyor belts are usually stretched by a preload of about 0.1-0.5% of the initial belt length in order to avoid slipping at the deflection pulley. Therefore, the mounting concept needs to be able to hold out this change of the length during operation. Due to an induction of eddy currents into the secondary elements, a heat development of up to 125 °C can occur. Thus, the mounting concept must have a temperature resistance up to this temperature. The main task of the mounting concept is the compensation of occurring forces. Depending on the geometrical alignment of the secondary elements to the stator part, unbalanced normal forces can occur, which causes stress momentum and supports unwanted tilting.

As result of the previously mentioned requirements, several mounting concepts are developed and benchmarked concerning their fulfilment requirements. The most promising solution, which is depicted in Figure 11, is then selected in cooperation with a conveyor belt manufacturer.

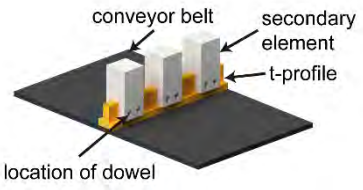


*Fig. 11 T-shaped mounting concept*

Here, a continuous t-shaped section is welded lengthwise on the textile bottom side using ultrasonic welding. Thus, the height of the secondary elements is extended and a groove is carved into the elements in order to position them by form-fit on the t-section. The efficiency of the stator part is also not influenced negatively by the height extension of the secondary elements. The form-fit mounting of the secondary elements is realized by using dowels, which are applied crosswise to the conveying direction. Two dowels are applied to each secondary element in order to increase the stiffness and to avoid possible tilting effects. For the quantification of the mechanical suitability of the mounting concept, several tests are conducted, which are presented in the following. The minimum requirements of the mechanical characteristics are assumed for the worst operation scenario, in which the full feed force is applied to the secondary elements caused by a blockade. Concerning this opera-

tion scenario, the force applied to a single secondary element amounts to 200 N.

In order to quantify the connection between the t-shaped profile and the secondary elements, tensile tests are conducted with two different profile materials. Table 2 shows the results of the tensile tests, which determine the limit of the possible load until the connection fails. The test is thereby based on DIN 53504 for the testing of rubber in a tensile test.

In summary, the tensile tests are conducted with two different profile materials at two stress configurations each. Concerning the first configuration, the t-profile is clamped one-sidedly and stress is applied on the secondary element in the direction of the force vector *F* with constant movement speed.

| **Stress** | ***Material of t-profile*** | $F_{e,max}$ **in N** | $F_{p,O}$ **in N** |
|---|---|---|---|
| 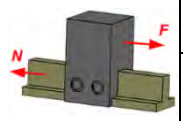 | Polyester | 300 | 420 |
| | Polyurethane | 450 | 600 |
| 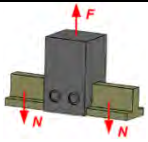 | Polyester | 270 | 490 |
| | Polyurethane | 450 | 1000 |

*Tab. 2 Results of the tensile tests*

Thus, on the one hand it is possible to determine the elastic area $F_{e,max}$ of both t-profile materials, for which the elongation effect is entirely reversible when retracting the stress. The plastic area $F_{p,O}$ marks the upper limit, from which a full, plastic failure occurs. Concerning the second configuration, the t-profile is clamped on both sides while stress is applied on the secondary elements vertically to the conveying direction. The results show that the material polyurethane is superior to the material polyester in both the elastic area and the area of plastic failure. Despite the failure of both materials, the dowels themselves stay intact. Furthermore, the results show that the assumed 200 N of applied force on a single secondary element leads only to elastic deformation. Thus, it can be assumed that the connection between the secondary elements and the t-section will not be damaged when applying the maximum load in the worst case.

In order to be able to make a statement about the stress resistance of the connection between the t-profile and the conveyor belt, the cohesion strength of the layers between the t-profile and the conveyor belt is tested on the basis of DIN 53530. The reachable cohesion strength of a welded connection is depending on the manufacturing parameters as well as the texture of the conveyor belt and the t-profile. Despite the fact that different t-profile materials have been used, the results are comparable. Due to the welding process, the fabric structure of the conveyor belt was transferred on to the underside of the t-profile. The damage is characterized by long fibers, which indicates that the textile plain weave has been ripped out locally. The adhesion of the short fibers can be found in corresponding, undamaged areas of the conveyor belt. Thus, as result a minimum cohesion strength of 96 N is achieved for all t-profile materials with a base width of 12 mm. Therefore, the connection between t-profile and conveyor belt depicts a layer cohesion strength of 8 N/mm. This value is above the minimum cohesion strength value of 4 N/mm set by the manufacturer for similar pairs of material.

As summary it can be concluded that, concerning the mechanical characteristics, the presented concept for lengthwise welded t-profiles is suitable to positively connect the secondary elements with the conveyor belt and to withstand to occurring forces. The temperature resistance was tested up to 125 °C by applying static stress. There were neither deformations of the material nor losses of the mechanical characteristics observed. The compliance with the pole pitch is depending on the accurate distances of the drill holes for the dowels. A constant pole pitch can be achieved with an adequate manufacturing precision. Section 3.1 proves that for an optimum force transmission, the biggest possible ratio $k_B$ is desired. Due to the fixed belt width $B_T$, the width of the force transmission $B_L$ is to be maximized. The base width of the chosen t-section, which is made through an extrusion process, can be extended without negatively influencing the operational behavior. Depending on the application, the base width can be varied in a later step in order to achieve an optimum ration between the manufacturing costs and the force transmission characteristic.

## 4 INTERFACE: MOTOR AND SECONDARY ELEMENTS

Apart from a sufficiently dimensioned interface between the conveyor belt and the secondary elements, the design of an adequate guidance system between stator part and secondary elements is required in order to minimize the frictional influence between these two objects.

Due to the magnetization of the stator (see Figure 4), a magnetic normal force component occurs additionally to the reluctance force. A double-sided design of the stator principally

leads to a situation, in which the normal forces between the secondary element and the respective stator compensates each other in the form of an unstable balance. In order to achieve a full compensation, it is necessary to position the secondary elements directly in the center. However, this is not possible due to tolerances of an economical justifiable manufacturing process. According to the design, the hybrid motor has a theoretical air gap of 0.6 mm on both sides. From the manufacturing point of view, however, the gap deviates from this by ± 0.1 mm due to the design, which consists of stacked electrical sheets. If the secondary element deviates from the ideal central position, the standard force increases strongly linear in concordance with the deviation. Figure 12 shows the correlation of the resulting normal force in dependence of the secondary element's deviation from the central position.

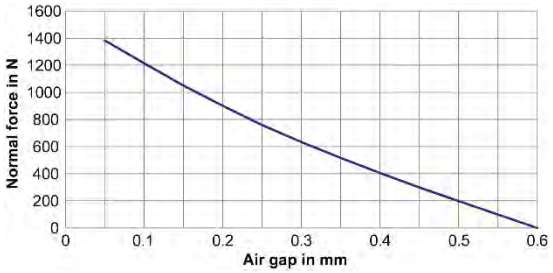


*Fig. 12 Normal force progression of the hybrid motor*

Assuming an one sided air gap of i.e. 0.2 mm, the simulative results, which have been proven by tests, show the influence of a normal force of 930 N on the secondary elements. Therefore, the chosen double-sided design also indispensably requires a guidance. In the course of the investigations, guidance concepts are developed, which are prototypically implemented into the hybrid motor. Figure 13 shows a section of the hybrid motor with the respective guidance concepts. The moving direction of the secondary elements is into or out of the picture plane, which is depending on the direction of the moving electromagnetic field created by the frequency converter.

Concerning guidance concept 1, virgin polytetrafluorethylene (PTFE) is used as sliding component on both sides. With this, the secondary elements are supported at the upper and lower edges inside the hybrid motor.

Advantages of this concept is the simple design and the anticipated low friction loss, which generally depends on the slide pairing of the secondary element's material and the slide surface. The slides are mounted on adjustable devices, in order to be able to vary the gap between the slide and the secondary elements during the test realization. In order to arrange the secondary elements centrically when entering the effective area of the motor, a suitable transition area is necessary at the slides, which is achieved through roundings. This is done in order to avoid an increased friction stress or blockade at the point when entering the motor. Especially the low adhesive capability can be seen as an advantage from the technical point of view, as it results in a low friction between PTFE and other materials.

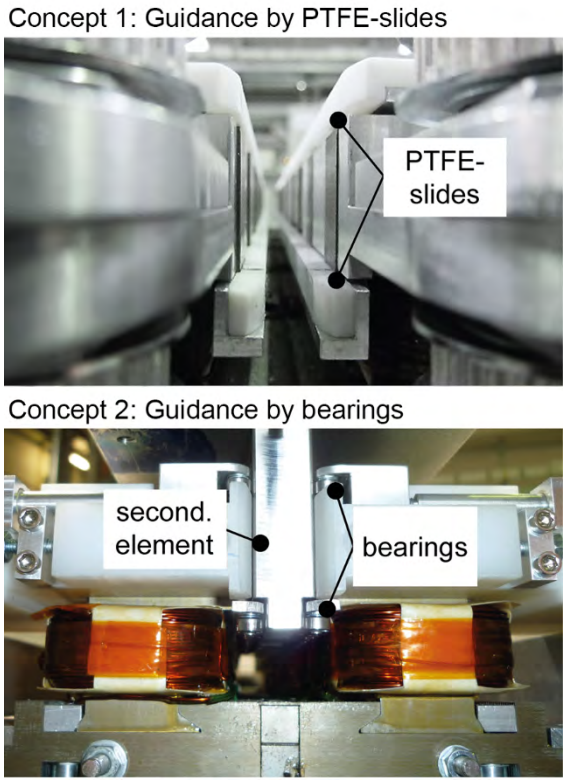


*Fig. 13 Guidance concepts*

The friction coefficient of the materials steel/PTFE can be assumed for a very low speed of $\mu_G$(steel/PTFE) = 0.05. At a speed of v ≈ 0.8 m/s the slide-friction coefficient approaches $\mu_G$(steel/PTFE) ≈ 0.25. In addition, the coefficients of PTFE are identical for dynamic and static friction. Thus, no stick-slip effect occurs. The friction losses of the PTFE slides are caused by the secondary elements sliding through the motor on the slides. Although it is possible to find very detailed information concerning the slide-friction characteristics of steel/PTFE in literature, this coefficient is, apart from the speed, additionally depending on the surface pressure. [14] Therefore it is only possible to determine the friction losses through practical measurement results.

The forces, which are required to move the secondary elements through the motor, were determined through a fixed plate equipped with secondary elements on the top. The friction losses per section amounts to 25 N for a speed

of 0.05 m/s. Approximated to the entire length of the motor, a friction loss of 154 N can be determined. This corresponds to about 88 % of the provided power of the hybrid motor. At a higher speed, the slide-friction coefficient of PTFE to steel increases. Therefore, this guidance concept is not suitable to achieve the desired conveying speed of 2 m/s.

The second guidance concept is based on small grooved ball bearings, which are integrated along the top and bottom edge of the sections in a continuous line. The ball bearings are mounted on a common rail, which is used to adjust the air gap to the secondary elements. For first tests, rails with each consisting of 14 ball bearings are used in order to ensure a guidance within the motor section. The hybrid motor consists of six motor sections. Within a section, two stator pairs are located. The ball bearing guidance achieves a friction loss of 2.5 N for one section when using a feed force of 0.05 m/s. Approximated to the entire hybrid motor, the loss amounts to 15.4 N. This corresponds to 8.8 % of the provided feed force of 175 N. The disadvantage of this guidance concept is the installation position change of the motor, which results in an elevation of the design of 7 mm. A further disadvantage are the high costs of the ball bearings as the price of the ball bearings for each section is around 400 EUR considering the current market price. However, the durability of the ball bearings is advantageous as they are operated far below the nominal range given by the manufacturer. Thus, low wear is to be expected. This concept is used for the evaluation in the next section.

## 5 EVALUATION

For evaluation purposes, a demonstrator was designed and built including the proposed interface solutions. Figure 14 shows the realized belt conveyor with the embedded hybrid motor (not visible) in the top-run and the corresponding secondary elements that are mounted on the conveyor belt's running side.

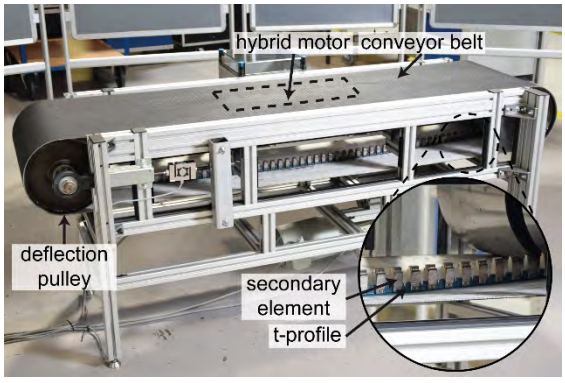


*Fig. 14 Demonstrator with hybrid motor*

As material for the secondary elements, pure iron was selected. With an iron content of min. 99.85 %, it has excellent magnetic properties as well as an improved resistance against corrosion and oxidation in comparison to normal steels.

First measurements under different test setups were performed in order to quantify the influence of single components concerning friction loss. Due to missing position feedback of the secondary elements, the hybrid motor was operated in stepper mode by applying a user-defined frequency, peak and continuous current. In this mode a successful movement of the conveyor belt was registered at a continuous current of 3 A within a speed range of 0.1-1.0 m/s. For this configuration, an overall mean value of 157.1 N was determined, which represents the force transmission from the hybrid motor into the conveyor belt. The influence of the guidance by bearings amounts to 127.1 N, which differs from the expected value of 15.4 N. The main reason for such a big deviation can be found in the fabrication tolerances of the hybrid motor. Because of the external fabrication and the use of laminated steel sheets, the geometrical tolerances amount to 0.2-0.7 mm over the motor length. As result, the setting of the guidance is a compromise between compensation of the geometrical tolerances and proper guiding in order to reduce the permanent magnetic influence.

Investigations concerning the temperature have shown that the windings of the motor reach a maximum value of 91.3 °C with an asymptotic behavior. For a continuous current of 3 A the motor will not reach a value of more than 125 °C.

## 6 SUMMARY

The objective of this study was the development of an alternative drive concept for conveyor belt systems. Thus, a linear direct drive was developed, which makes it possible to transmit the feed forces into the conveyor belt along the complete motor length. In contrast to conventional drive systems, it is possible to reduce the conveyor belt pretension as well as the load peaks in the conveyor belt when using a driven pulley.

A linear direct drive was developed on the basis of the hybrid motor, which combines the advantages of the high efficiency of permanent-magnet-excited machines with the principles of the reluctance motors. Concerning this motor concept, the permanent magnets can be installed in the fixed stator part of the motor.

In order to enable the operation of a linear direct drive with flexible conveyor belts, the investigation of the force transmission path from the motor to the conveyor belt is required. For a practical depiction, the finite-element-method was used. Using a multi scale approach it is possible to model the conveyor belt on the basis of elementary cells stringed together, which depicts the characteristics of the entire conveyor belt due to its periodic structure. On the basis of this model, the force transmission can be depicted for different drive concepts from the motor into the conveyor belt when conveying a single piece good. From the simulation of different mounting principles of secondary elements on to the conveyor belt, it can be concluded that the width of the force transmission needs to be maximized in order to achieve an optimum force progression. Based on this result, a solution concept was developed, in which the secondary elements are connected with the conveyor belt through an intermediate t-shaped profile. Mechanical investigations show that the presented concept is suitable for use in the linear motor operation.

Furthermore, the interface between the conveyor belt and the secondary elements was investigated. Simulations, which were supported by measurements, show that a deviation from the central position of the secondary elements results in a significant increase of lateral working normal forces. In the course of this study, two different guidance concepts were developed, which are prototypically implemented in the hybrid motor. Here, the best results are shown by the guidance concept, in which ball bearings compensate the lateral deviation of the secondary elements.

First measurements on a demonstrator with the implemented hybrid motor and the corresponding conveyor belt with secondary elements were conducted. When applying a current of 3 A, the demonstrator is able to provide a permanent feed force of 157.1 N without the need for further cooling. Within the scope of this study, it was possible to show, which technical problems need to be solved concerning the linear motor drive. Further investigations on the demonstrator are in focus of the next steps.

## 7 REFERENCES

[1] Wagner, G. et al.: Fördertechnik: Grundlagen. In: Grote, K.-H. (Hrsg.); Feldhusen, J. (Hrsg.): Dubbel – Taschenbuch für den Maschinenbau. Springer-Vieweg, 2014.

[2] Westkämper, E.; Löffler, C.: Strategien der Produktion: Technologien, Konzepte und Wege in die Praxis. Springer-Vieweg, 2016.

[3] Martin, H.: Transport- und Lagerlogistik: Planung, Struktur, Steuerung und Kosten von Systemen der Intralogistik. Springer-Vieweg, 2014.

[4] Jodin, D.; Hompel, M. ten: Sortier- und Verteilsysteme: Grundlagen, Aufbau, Berechnung und Realisierung. Springer, 2012.

[5] Vierling, A.: Zur Theorie der Bandförderung. Bd. 8. Continental-Transportband-Dienst, 1972.

[6] Radosavac, M.; Froböse, T.; Overmeyer, L.; Jastrzembski, J.-P.; Ponick, B.: Lineardirektantrieb für Transportbänder. In: Proceedings. Logistics Journal, Vol. 7, 2011.

[7] Koster, K: Leichttransportbandtechnik. Vulkan-Verlag Essen, 1989.

[8] Hötte, D.; Overmeyer, L.: Längere Förderstrecken dank antreibender Tragrollen, phi – Produktionstechnik Hannover informiert, Nr. 12, 2016.

[9] Alles, R.: Zum Zwischenantrieb von Gurtförderern mittels angetriebener Tragrollen und Linearmotoren. Dissertation der Fakulatät für Maschinenwesen der Technischen Universität Hannover, 1976.

[10] Radosavac, M.; Overmeyer, L.: Development of a Linear Direct Drive for Conveyor Belts. In: Logistics Journal, Vol. 2016, 2016.

[11] Jastrzembski, J.-P.: Synchrone Linear-Direktantriebe für Förderbänder. Fortschritt-Berichte VDI Düsseldorf, 2014.

[12] Rolfes, R. et al.: Material and Failure Models for Textile Composites. In: Camanho, P. P. et al. (Hrsg.): Mechanical response of composites. Springer, Berlin, 2008.

[13] Balke, H.: Einführung in die Technische Mechanik: Festigkeitslehre. Springer-Vieweg, 2014.

[14] Domininghaus, H. et al.: Kunststoffe: Eigenschaften und Anwendungen. Springer-VDI, 2012.

| | |
|---|---|
| Authors: | Radosavac, Mišel<br>Overmeyer, Ludger |
| University | Leibniz Universität Hannover |
| Department: | Institute of Transport and Automation Technology (ITA) |
| E-mail: | misel.radosavac @ita.uni-hannover.de<br>ludger.overmeyer @ita.uni-hannover.de |